Molecular Vision 2021; 27:161-178 <http://www.molvis.org/molvis/v27/161>
Received 2 April 2020 | Accepted 31 March 2021 | Published 2 April 2021

NADPH oxidase–induced oxidative stress in the eyes of hypertensive rats

Álvaro Santana-Garrido,[1,3] Claudia Reyes-Goya,[1] Carmen Fernández-Bobadilla,[1] Antonio J. Blanca,[1] Helder André,[2] Alfonso Mate,[1,3] Carmen M. Vázquez[1,3]

[1]Departamento de Fisiología, Facultad de Farmacia, Universidad de Sevilla. CL Profesor García González, Sevilla, Spain; [2]Department of Clinical Neuroscience, St. Erik Eye Hospital, Karolinska Institutet, Stockholm, Sweden; [3]Epidemiología Clínica y Riesgo Cardiovascular, Instituto de Biomedicina de Sevilla (IBIS), Hospital Universitario Virgen del Rocío – Consejo Superior de Investigaciones Científicas – Universidad de Sevilla. Avda. Manuel Siurot s/n, Sevilla, Spain

Purpose: Increased reactive oxygen species (ROS) released by NADPH oxidase and inflammation are associated with arterial hypertension and eye diseases associated with high blood pressure, including glaucoma, retinopathies (e.g., age-related macular degeneration), and choroidopathies affecting ocular function; however, the mechanisms underlying these adverse outcomes remain undefined. The present study was designed to highlight the importance of oxidative stress in severe hypertension-related eye damage.

Methods: Male Wistar rats (n = 7, unless otherwise specified for specific experiments) were administered an oral dose of 30 mg of Nω-nitro-L-arginine methyl ester (L-NAME) per kilogram of bodyweight and day for 3 weeks; chronic administration with L-NAME is a validated experimental approach resulting in severe hypertension secondary to nitric oxide (NO) depletion and subsequent vasoconstriction in the systemic circulation. Upon treatment completion, histomorphometric studies, NADPH oxidase activity, and ROS production were measured in eyecup homogenates and paraffin-embedded sections from control and L-NAME-treated animals. In addition, immunohistofluorescence, western blotting, and real-time PCR (RT-qPCR) analyses were performed in the eye and the retina to evaluate the expression of i) NADPH oxidase main isoforms (NOX1, NOX2, and NOX4) and subunits (p22phox and p47phox); ii) glial fibrillary acidic protein (GFAP), as a marker of microglial activation in the retina; iii) antioxidant enzymes; and iv) endothelial constitutive (eNOS) and inflammation inducible (iNOS) nitric oxide synthase isoforms, and nitrotyrosine as a versatile biomarker of oxidative stress.

Results: Increased activity of NADPH oxidase and superoxide anion production, accompanied by transcriptional up-regulation of this enzyme isoforms, was found in the retina and choroid of the hypertensive rats in comparison with the untreated controls. Histomorphometric analyses revealed a significant reduction in the thickness of the ganglion cell layer and the outer retinal layers in the hypertensive animals, which also showed a positive strong signal of GFAP in the retinal outer segment and plexiform layers. In addition, L-NAME-treated animals presented with upregulation of nitric oxide synthase (including inducible and endothelial isoforms) and abnormally elevated nitrotyrosine levels. Experiments on protein and mRNA expression of antioxidant enzymes revealed depletion of superoxide dismutase and glutathione peroxidase in the eyes of the hypertensive animals; however, glutathione reductase was significantly higher than in the normotensive controls.

Conclusions: The present study demonstrated structural changes in the retinas of the L-NAME-treated hypertensive animals and strengthens the importance of NADPH oxidase as a major ROS-generating enzyme system in the oxidative and inflammatory processes surrounding hypertensive eye diseases. These observations might contribute to unveiling pathogenic mechanisms responsible for developing ocular disturbances in the context of severe hypertension.

The inability of antioxidant defense mechanisms to counteract reactive oxygen species (ROS) formation, which typically defines oxidative stress, is known to cause tissue damage, cell death, and acceleration of the aging process. Oxidative imbalance and inflammatory processes have been attributed a major role in the pathogenesis of various systemic and eye diseases, including age-related macular degeneration (AMD), corneal and conjunctival disorders, glaucoma, retinitis pigmentosa, and different types of retinopathies, among others [1].

As the eye is highly vascularized, and because the retina is a sensorineural tissue that can be especially affected by high blood pressure, it is not surprising that arterial hypertension (AH) is a risk factor for several vision-threatening eye conditions, including cataract [2-4], glaucoma [5], choroidopathies [6], AMD [7], and hypertensive and diabetic retinopathies [8]. However, and despite previous reports describing harmful effects on the eye as a target of AH, the

Correspondence to: Alfonso Mate, Departamento de Fisiología, Facultad de Farmacia, Universidad de Sevilla, CL Profesor García González 2, 41012 Sevilla, Spain. Phone: +34 954 556 518; email: mate@us.es

precise mechanisms responsible for eye dysfunction in this context remain unknown.

Previous reports support the notion that the enzyme NADPH oxidase has a pivotal role in ROS production (mainly the superoxide anion ($O_2^{\cdot-}$) and/or H_2O_2) and subsequent organ damage in the hypertensive context [9,10]. Seven isoforms of the catalytic subunit of this enzyme complex (NOX1–5 and Duox1–2) have been characterized thus far and are differentially expressed in various tissues [11]. The isoform NOX4 was recently subdivided into NOX4A and NOX4B [12], which seem to differ in terms of tissue-specific expression and overall function. The predominant NOXes in vascular cells are isoforms NOX1, 2, 4, and 5, yet the implications of the latter in hypertension and cardiovascular disease remain obscure at present [13].

$O_2^{\cdot-}$ is released mainly by NOXes 1, 2, 3, and 5, whereas NOX4 and Duox1–2 generate H_2O_2 prominently [14]. Independently of the precise mechanisms responsible for ROS production via NADPH oxidase, sustained oxidative stress can disturb the generation of nitric oxide (NO) from endothelial nitric oxide synthase (eNOS), thus leading to uncoupling of the latter that results in extra $O_2^{\cdot-}$ production and perpetuates the situation. This would eventually lead to endothelial dysfunction and neovascularization, because NO helps maintain ocular hemodynamics by protecting the endothelial cells of vascular beds and nerve fibers against pathogenic processes, for example, diabetes mellitus and glaucoma [15,16].

Several studies have postulated the possible participation of NOX family proteins in different eye pathologies. For instance, NOX2 has been involved in the functional alterations observed in the retina under experimental conditions mimicking diabetes and glucolipotoxicity [17], and the role of NOX4 has recently been shown in retinal vascular diseases [18]. In addition, NOX4 is an indicator of oxidative damage in retinoblastoma tumors [19], promotes neovascularization following O_2-dependent retinopathy [20], and is involved in the development of retinopathies, such as AMD [21-24]. Regarding other ocular structures, ROS production by NOX1, NOX4, and NOX5 has been detected in corneal stromal cell cultures [25], and NOXes have been involved in experimental corneal neovascularization [26].

Excessive ROS production can also lead to an imbalance in the inflammatory process, thus playing a decisive role in the development of ocular diseases. In this sense, retinal inflammation has been associated with many ocular diseases, including diabetic retinopathy [27] and AMD [28]; and microglial activation has been observed in the retinas of spontaneously hypertensive rats when compared with normotensive animals [28]. All these findings support the hypothesis that NOX isoforms are implicated in the origin or progression or both of many ocular pathologies, thus suggesting an association among oxidative stress, NADPH oxidase, inflammation, and hypertensive ocular disorders.

N(ω)-nitro-L-arginine methyl ester (L-NAME) is a well-known compound used to examine the pathophysiology and therapeutics of AH [29]. Chronic exposure to L-NAME favors prolonged vasoconstriction due to competitive inhibition of eNOS and subsequent reduction of NO formation. Eventually, L-NAME causes persistent hypertension that is associated with damage to different organs [30] including the eye [31,32]. Therefore, rats with hypertension induced by NO depletion constitute a validated experimental model to increase our knowledge of high blood pressure–related ocular disorders.

The main objective of this study was to assess the role of oxidative stress among the mechanisms responsible for ocular damage in a rodent model with chronic arterial hypertension. To this end, morphometric studies, estimation of ROS levels and the activity and location or expression of NOX components, as well as the expression of nitric oxide synthase (inducible and endothelial isoforms), nitrotyrosine, and antioxidant enzymes (superoxide dismutase, glutathione peroxidase, and glutathione reductase), were determined in eyecups obtained from Wistar rats subjected to L-NAME-treated hypertension. In addition, the location and quantification of glial fibrillary acidic protein (GFAP) were investigated in retinal layers as a marker of local microglia activation.

METHODS

Experimental design: The study was performed in accordance with the European Union (EU Directive 2010/63/EU) and national (RD 53/2013) guidelines for the care and use of laboratory animals and was approved by the competent experimentation ethics committee at the University of Sevilla, Spain, where the animal work took place (approval reference # 22/10/2018/148, issued by Junta de Andalucía, Dirección General de la Producción Agraria y Ganadera). The study was also in accordance with the Association for Research in Vision and Ophthalmology (ARVO) Statement for the Use of Animals in Ophthalmic and Vision Research. Ten- to 12-week-old male Wistar rats housed with free access to food and drink and exposed to 12 h:12 h light-dark cycles were randomly assigned into two groups (n = 7 in both cases, unless otherwise stated). The hypertensive group was established by treating the animals with 30 mg L-NAME/kg bodyweight/day p.o. for 3 weeks. The concentration of L-NAME in the drinking water was calculated weekly considering the

evolution of bodyweight and water intake. The control group was subjected to the same conditions except the absence of L-NAME in the feeding bottles.

Blood pressure measurements: On a weekly basis, systolic blood pressure (SBP) was estimated with the noninvasive tail-cuff technique with a pressure recorder (NIPREM 645; Cibertec, Madrid, Spain). SBP was calculated as the average of three to four consecutive records.

Histomorphometric studies: Intravitreal injections of 4% paraformaldehyde (PFA) in PBS (1X; 137 mM NaCl, 2.7 mM KCl, 10 mM Na_2HPO_4, 1.8 mM KH_2PO_4, pH 7.4) were administered in the eyecups of deeply anesthetized animals (75 mg/kg ketamine plus 10 mg/kg diazepam, i.p.) before enucleation. Then, the eyeballs were post-fixed in 4% PFA for 24 h, and subsequently processed for paraffin embedding. Five micron sections were obtained with a manual rotatory microtome (MR2258; Histo-Line Laboratories, Milan, Italy) and stained with hematoxylin and eosin (H&E) for histomorphometric studies. H&E images were acquired using an Olympus BX41 microscope coupled to an Olympus DP73 camera (Olympus Iberia, Barcelona, Spain). The relative thickness of the retinal layers was measured as previously described [33], using ImageJ-NIH freeware (v. 2.0.0).

Ocular enucleation and homogenization: Upon completion of treatment, the rats were anesthetized with 75 mg/kg ketamine and 10 mg/kg diazepam (i.p.). Both eyes were enucleated as described [34] and collected in a Petri dish containing Krebs solution. The cornea, lens, and vitreous body were discarded following corneal incision under a binocular stereoscopic microscope into eyecups containing retina/RPE/choroid/sclera complexes. Each eyecup was subdivided into portions that were snap-frozen in liquid nitrogen and maintained at −80 °C before homogenization.

One portion of both eyecup samples was homogenized in protease inhibitor–containing 50 mmol/l phosphate buffer (pH 7.4). After immediate centrifugation (10,000 ×*g*, 10 min), the protein-containing supernatant was used for determining NADPH oxidase activity and protein concentration [35]. The remaining portion of both eyecups was maintained at −80 °C for mRNA isolation and gene expression analyses.

Measurement of NADPH oxidase activity and ROS levels: The activity of NADPH oxidase was determined as previously described [36]. Briefly, a volume equivalent to 100 µg proteins from the eyecup homogenates was placed on a single-tube luminometer and mixed with 5 µmol/l lucigenin and 0.1 mmol/l NADPH. The chemiluminescence reaction was continued for 4 min, and values were expressed as percentages over the normotensive control group. To characterize the source of superoxide anion, the samples were preincubated with 0.1 mmol/l of oxypurinol, rotenone, or diphenyleneiodonium (DPI), respective inhibitors of xanthine oxidase, complex I of the electron transport chain, and flavoenzymes, such as NOXes and Duoxes.

Additional experiments (n = 4 animals per group) were performed to measure $O_2^{\cdot-}$ and the location of the NADPH oxidase isoforms in the retinal layers. For this purpose, 5-µm paraffin sections were obtained as described previously and further processed to estimate $O_2^{\cdot-}$ by using dihydroethidium (DHE; Cat. No. HY-D0079; MedChemExpress, Monmouth Junction, NJ) as a fluorescent dye. This molecule specifically reacts with intracellular superoxide anion and turns into red fluorescent ethidium in nuclei. Deparaffinized sections were incubated with DHE for 20 min at 37 °C, as previously described [37]. Then, sections were mounted with 4′,6-diamidino-2-phenylindole (DAPI) Fluoromount-G® (Cat. No. 0100–20; SouthernBiotech Associates, Inc., Birmingham, AL) and photographed under similar exposure conditions using a fluorescence microscope (Olympus DP73, Tokyo, Japan). The intensity of the staining was measured using ImageJ software (version 2.0.0).

RT–PCR: Eyecup samples were subjected to the TRIzol total RNA isolation protocol (Thermo Fisher Scientific, Madrid, Spain) followed by reverse transcription as previously reported [38]. Gene products (*NOX1, NOX2, NOX4, p22phox, p47phox, SOD, GSH-Red,* and *GSH-Px*) were amplified with a CFX96 real-time PCR System (Bio-Rad, Madrid, Spain) and using the specific primers summarized in Table 1. iTaq™ Universal SYBR® Green Supermix (BioRad, Madrid, Spain) reactions were initiated by activation of iTaq™ DNA polymerase (95 ºC, 3 min) followed by 40 cycles of denaturation (95 ºC, 15 s) plus annealing/extension (60 ºC, 30 s). Housekeeping gene *GAPDH* was used as an internal control.

Western blotting analyses: Thirty to sixty microns of proteins from the eyecup homogenates were subjected to gel electrophoresis and identified with relevant antibodies (anti-NOX1, anti-NOX2, anti-NOX4, anti-p22phox, anti-p47phox, anti-eNOS, anti-iNOS, anti-nitrotyrosine, anti-SOD, anti-GSH-Red, and anti-GSH-Px), as previously described [39]. In turn, GFAP expression was measured in a similar manner using a mouse monoclonal anti-GFAP in the retina homogenates (see Table 2 for antibody sources and dilutions). All immunoblots were analyzed with an Amersham Imager 600 blot and gel imager (Cytiva, Sheffield, UK), and the GAPDH protein was chosen as a loading control.

Immunohistofluorescence: Deparaffinized eye sections, obtained as described, were also used to evaluate NOX expression with immunohistofluorescence staining. Briefly,

Table 1. Primers used for real-time PCR.

Gene	Forward primer (5′–3′)	Reverse primer (5′–3′)
NOX1	TTCACCAATTCCCAGGATTGAAGTGGATGGTC	GACCTGTCACGATGTCAGTGGCCTTGTCAA
NOX2	CCCTTTGGTACAGCCAGTGAAGAT	CAATCCCACGTCCCACTAACATCA
NOX4	TTGCTTTTGTATCTTC	CTTACCTTCGTCACAG
p22phox	GCTCATCTGTCTGCTGGAGTA	ACGACCTCATCTGTCACTGGA
p47phox	GCTCACCGAGTACTTCAACA	GCCTTCTGCAGATACATGGA
SOD	CGTCATTCACTTCGAGCAGAAGG	GTCTGAGACTCAGACCACATA
GSH-Red	GGAAACTCGCCCATAGACTT	CCAACCACCTTCTCCTCTTT
GSH-Px	GGAGAATGGCAAGAATGAAGA	CCGCAGGAAGGTAAAGAG
GAPDH	GCCAAAAGGGTCATCATCTCCGC	GGATGACCTTGCCCACAGCCTTG

sections were processed for antigen retrieval with Diva Decloaker (Biocare Medical, LLC, Pacheco, CA). The following primary antibodies were used for immunostaining: mouse monoclonal anti-NOX1 (C-10; 1:200 dilution; Santa Cruz Biotechnology, Santa Cruz, CA), rabbit monoclonal anti-NOX2 (1:100 dilution; Epitomics-Abcam, Burlingame, CA), rabbit monoclonal anti-NOX4 (1:500 dilution; Epitomics-Abcam), and mouse monoclonal anti-GFAP (1:200 dilution; Santa Cruz Biotechnology). Goat anti-mouse Alexa Fluor® 647 (Cat. No. CSA3808; Cohesion Biosciences Ltd., London, UK) and goat anti-rabbit Alexa Fluor® 555 (Cat. No. CSA3411; Cohesion Biosciences Ltd.) were used as a fluorescent secondary antibodies. Sections were mounted with DAPI Fluoromount-G®, and images were acquired on an Olympus DP73 color digital camera using a 10X objective and suitable excitation and emission filters for each antibody.

Statistical analyses: All results are expressed as mean ± standard error of mean (SEM). Unless otherwise stated, data were subjected to an unpaired Student *t* test using GraphPad InStat software (San Diego, CA) and considered statistically different at $p<0.05$.

RESULTS

Effect of L-NAME on bodyweight, blood pressure values, and retinal layer thickness: Three-week exposure to L-NAME did not affect the animals' weight (390±18.0 versus 390±9.00 for the control and L-NAME-treated rats, respectively). However, the SBP values were significantly increased from week 1 in the L-NAME-treated animals and appeared to plateau at week 3 when severe chronic hypertension was already established (191±3.00 versus 130±3.00 for the L-NAME-treated and control groups, respectively; Figure 1A).

Figure 1B shows representative images of H&E-stained retinas. Normal distribution and morphology of the retinal and RPE/choroid layers were observed in the normotensive controls and in the L-NAME-treated animals. However,

Table 2. Antibodies used for western blotting analyses.

Primary antibody	Origin	Dilution	Secondary Antibody	Dilution
Anti-NOX1	Mouse monoclonal	1:1000	Goat anti-mouse	1:2000
Anti-NOX2	Rabbit monoclonal	1:8000	Goat anti-rabbit	1:4000
Anti-NOX4	Rabbit polyclonal	1:1000	Goat anti-rabbit	1:2000
Anti-p22phox	Rabbit polyclonal	1:1000	Goat anti-rabbit	1:2000
Anti-p47phox	Rabbit polyclonal	1:1000	Goat anti-rabbit	1:2000
Anti-eNOS	Mouse monoclonal	1:2000	Goat anti-mouse	1:4000
Anti-iNOS	Mouse monoclonal	1:2000	Goat anti-mouse	1:4000
Anti-nitrotyrosine	Mouse monoclonal	1:1000	Goat anti-mouse	1:2000
Anti-GSH-Px	Rabbit polyclonal	1:2000	Goat anti-rabbit	1:4000
Anti-GSH-Red	Rabbit polyclonal	1:5000	Goat anti-rabbit	1:8000
Anti-SOD	Mouse monoclonal	1:1000	Goat anti-mouse	1:2000
Anti-GFAP	Mouse monoclonal	1:2000	Goat anti-mouse	1:4000
Anti-GAPDH	Mouse monoclonal	1:10000	Goat anti-mouse	1:20000

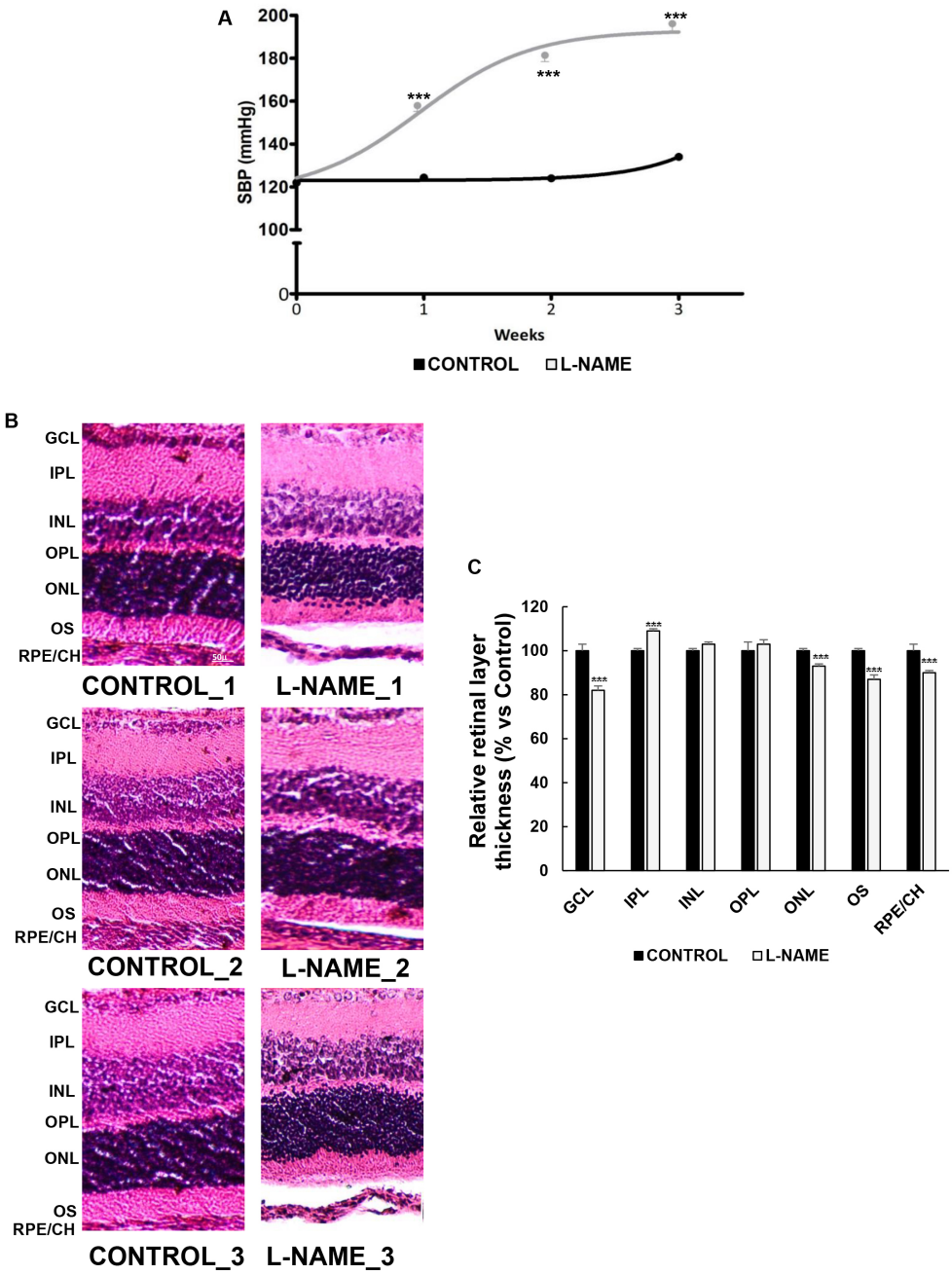

Figure 1. Effect of Nω-nitro-L-arginine methyl ester (L-NAME) on blood pressure and retinal layer thickness. **A**: Systolic blood pressure (SBP) values of rats receiving the standard control diet (black line) or subjected to treatment with L-NAME p.o. (gray line). **B**: Representative images of retinal sections subjected to hematoxylin and eosin staining (three images per group are shown as a representation of all animal samples processed). **C**: Histomorphometric analysis of relative retinal layer thickness. Plotted values are expressed as mean ± standard error of the mean (SEM) of seven animals per group. ***p<0.001 versus the CONTROL group.

significant reductions of 18%, 7%, 13%, and 10% were measured in the latter in the ganglion cell layer (GCL), outer nuclear layer (ONL), outer segments (OS), and RPE/choroid, respectively (Figure 1B,C). The inner plexiform layer (IPL) of the hypertensive retinas showed a 9% thickness increase compared with the control group.

NADPH oxidase activity and ROS levels: The activity of $O_2^{\cdot-}$-generating NADPH oxidase increased 2.34-fold in the eyecup homogenates from the hypertensive rats when compared with those of the normotensive controls (Figure 2A). To elucidate the source of the superoxide anions in the L-NAME-treated animals, we performed additional determinations in the homogenates preincubated with different inhibitors, as detailed. The fact that only DPI caused a major reduction in $O_2^{\cdot-}$ generation, while no changes were observed in samples exposed to oxypurinol or rotenone, suggests that the enhanced production of $O_2^{\cdot-}$ observed in the hypertensive animals resulted from increased activity of the enzyme NADPH oxidase (Figure 2B).

To check the levels of ROS generated in situ in the choroid and in specific retinal layers, we used DHE reactions (Figure 2C) to quantify and compare the intensity of fluorescence staining (Figure 2D) in the two experimental groups. The signal strength, which is proportional to superoxide production, was 1.6-fold higher in the L-NAME-treated rats in the ganglion cell layer, in the inner nuclear layer, and in the outer nuclear layer of the retinas. DHE staining increased also by 1.5-fold in the choroids from the hypertensive rats.

Gene expression of oxidative stress–related enzymes: To assess whether the observed increase in the activity of NADPH oxidase following L-NAME treatment correlated with changes in gene expression of this enzyme, we quantified the isoforms and subunits of the NADPH oxidase enzyme assayed in this study with real-time PCR. As shown in Figure 3, all analyzed elements revealed considerable increments of mRNA expression in the group subjected to L-NAME exposure (1.41-, 2.18-, 2.23-, 2.57-, and 1.62-fold for *NOX1, NOX2, NOX4, p22phox,* and *p47phox*, respectively, compared with the values measured in the normotensive group).

Antioxidant enzyme expression at the mRNA level is shown in Figure 4. *GSH-Px 1/2* and *SOD-1* were downregulated in the eyecups from the L-NAME-treated hypertensive rats (0.50- and 0.43-fold, relative to the control group, respectively; Figure 4A,C). Conversely, the expression of *GSH-Red* displayed a 1.36-fold increase after treatment with L-NAME (Figure 4B).

Protein expression analyses: To explore whether changes at the functional and mRNA levels also correlate with the protein expression pattern, we measured the relative abundance of NOX1, NOX2, NOX4, p22phox, and p47phox (Figure 5). NOX2 was increased 4.03-fold in the eyes from the hypertensive rats when compared with the control animals. The expression of the NOX1, NOX4, p22phox, and p47phox proteins was enhanced 1.62-, 1.48-, 2.48-, and 2.70-fold, respectively (Figure 5A–E).

Immunofluorescence analyses of NOX1, NOX2, and NOX4 were further performed in the retinal layers and the choroid (Figure 5F) to strengthen the results obtained in the immunoblotting analyses and to confirm the presence of the NOX protein in the different eye layers. All three isoforms of the NADPH oxidase enzyme were detected in the RPE/choroid (mostly localized around blood vessels) and the outer segment layers in both groups of animals, with a stronger signal in the hypertensive animals when compared with the control animals. NOX1, NOX2, and NOX4 were also detected in the outer plexiform layer from the hypertensive animals, and the latter displayed a signal in the inner plexiform layer, as well. In addition, NOX1 and NOX4 were slightly detected in the ganglion cell layer of the hypertensive rats but not in the control normotensive rats.

As the positive signal of the NOX isoforms in the plexiform layers might correspond to microglia activation, immunofluorescence of GFAP (a somewhat nonspecific response that reflects early retinal damage in different retinopathies) was performed in the retinal layers, and the relative abundance of this protein was then quantified with western blotting (Figure 5G). A faint GFAP signal could be observed only in the outer segment layer of the normotensive animals. However, GFAP staining appeared as a strong signal in the outer segment and the inner and outer plexiform layers from the hypertensive animals. These results were similar to a considerable increase (1.54-fold) in the protein expression of GFAP in the retina homogenates from the hypertensive animals in comparison with the untreated control rats.

Protein expression analyses of eNOS and iNOS displayed significantly higher expression for both enzymes (2.21- and 3.36-fold for eNOS and iNOS, respectively) in the rats subjected to L-NAME administration compared to the normotensive controls (Figure 6A,B). The additional marker of oxidative stress, nitrotyrosine, showed a 1.79-fold increase compared with the control animals (Figure 6C).

Regarding the protein expression of antioxidant enzymes, the results were similar to those obtained in the RT-qPCR experiments and showed reductions of 79% and 29%, respectively, in the amount of GSH-Px 1/2 and SOD-1 enzymes (Figure 7A,C), together with a 1.7-fold increase in

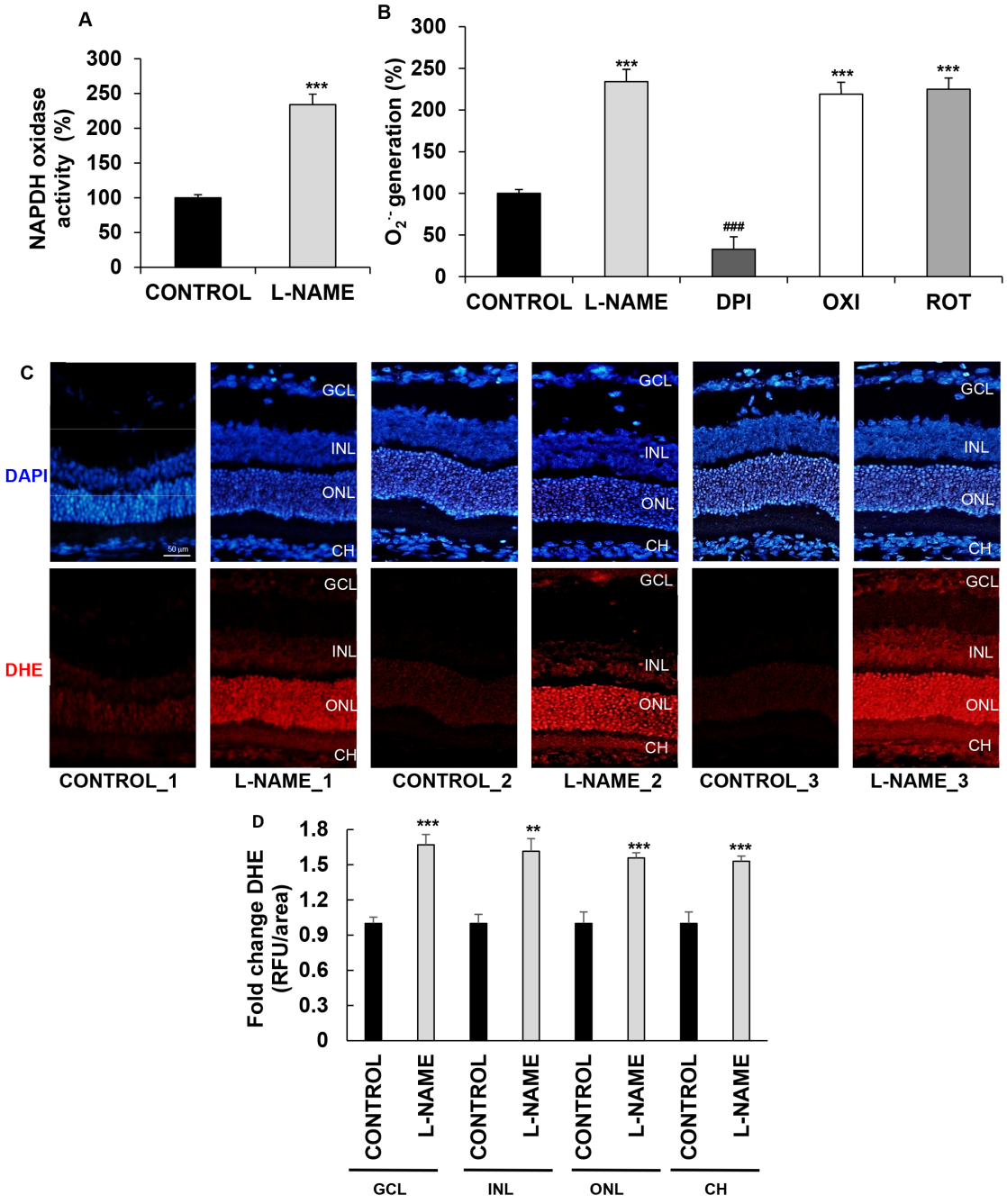

Figure 2. Effect of L-NAME on ROS production. **A**: NADPH oxidase activity in eyecup homogenates from normotensive (CONTROL) and hypertensive (Nω-nitro-L-arginine methyl ester, L-NAME) rats. Values are expressed as mean ± standard error of the mean (SEM) of seven animals per group. ***p<0.001 versus the CONTROL group. **B**: NADPH oxidase–mediated production of the superoxide anion. Eyecup homogenates from L-NAME-treated rats were used for NADPH oxidase chemiluminescence assay in the presence of 0.1 mM diphenyleneiodonium (DPI), oxypurinol (OXI), and rotenone (ROT) inhibitors. Values were subjected to one-way analysis of variance (ANOVA) followed by Tukey's multiple comparison posttest and are expressed as mean ± SEM of seven animals per group. ***p<0.001 versus the CONTROL group; ###p<0.001 versus the L-NAME group. **C**, **D**: Estimation of reactive oxygen species (ROS) levels in the retina and choroid with dihydroethidium (DHE) staining. **C**: DHE labeling (red) for ROS was present in the ganglion cell layer (GCL), in the inner nuclear layer (INL), and in the outer nuclear layer (ONL) of the retina, and in the choroid (CH), which can be distinguished with 4′,6-diamidino-2-phenylindole (DAPI, blue) nuclei staining. Three images per group are shown as a representation of all animal samples processed. **D**: Fluorescence intensity in (**C**) normalized to that of the CONTROL group in each corresponding layer, as quantified using ImageJ software. Plotted values are expressed as mean ± SEM of four animals per group: **p<0.01, ***p<0.001 versus the CONTROL group. RFU, relative fluorescence unit.

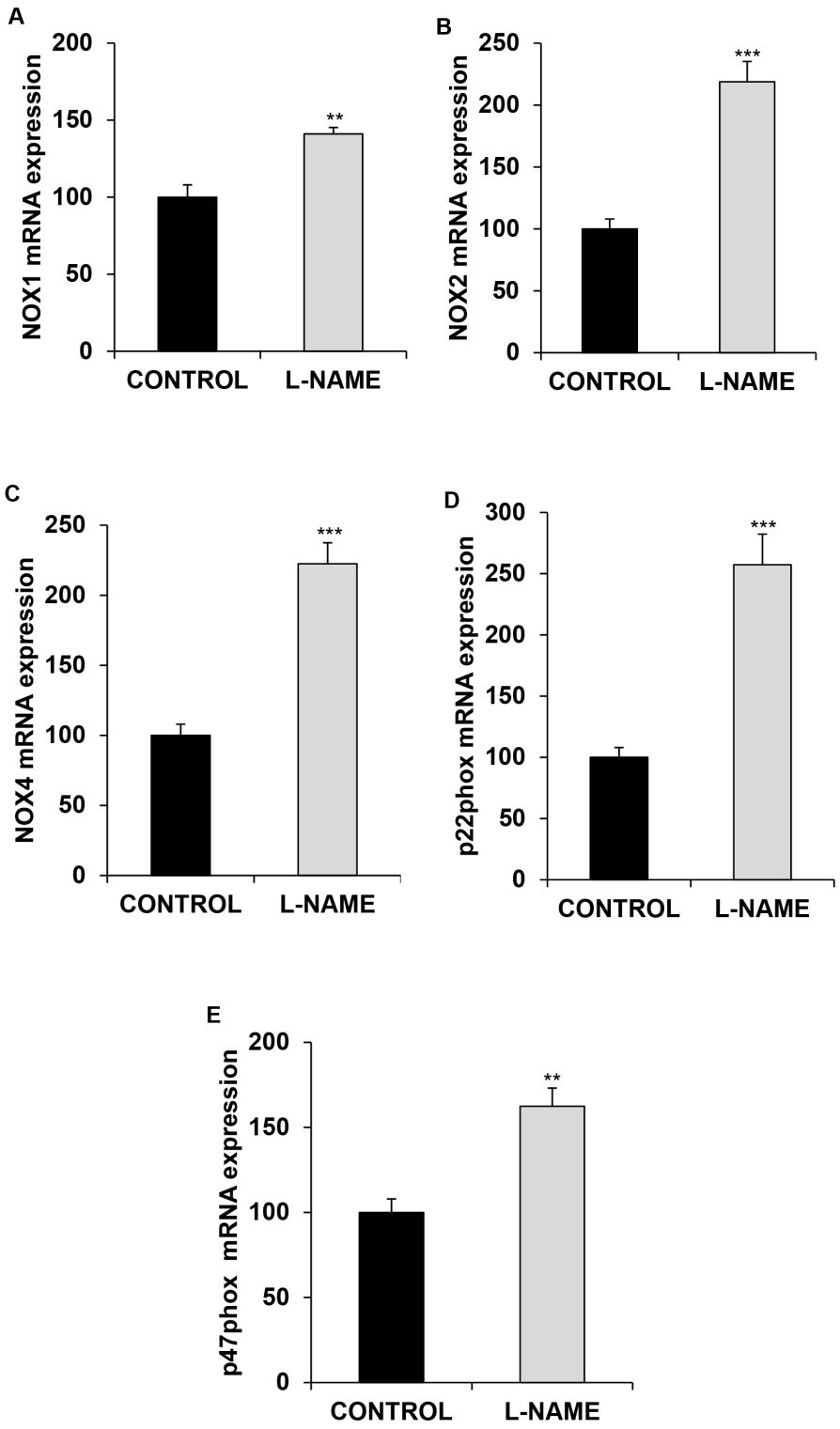

Figure 3. Gene expression of NADPH oxidase enzyme. Relative mRNA expression of (**A**) NOX1, (**B**) NOX2, (**C**) NOX4, (**D**) p22phox, and (**E**) p47phox, in the eyes of normotensive (CONTROL) and hypertensive (Nω-nitro-L-arginine methyl ester, L-NAME) rats. The quantitative fold changes in gene expression were determined as relative to *GAPDH* in each corresponding group and calculated using the $2^{-\Delta\Delta Ct}$ formula. Values are expressed as mean ± standard error of the mean (SEM) of seven animals per group. **p<0.01, ***p<0.001 versus the CONTROL group.

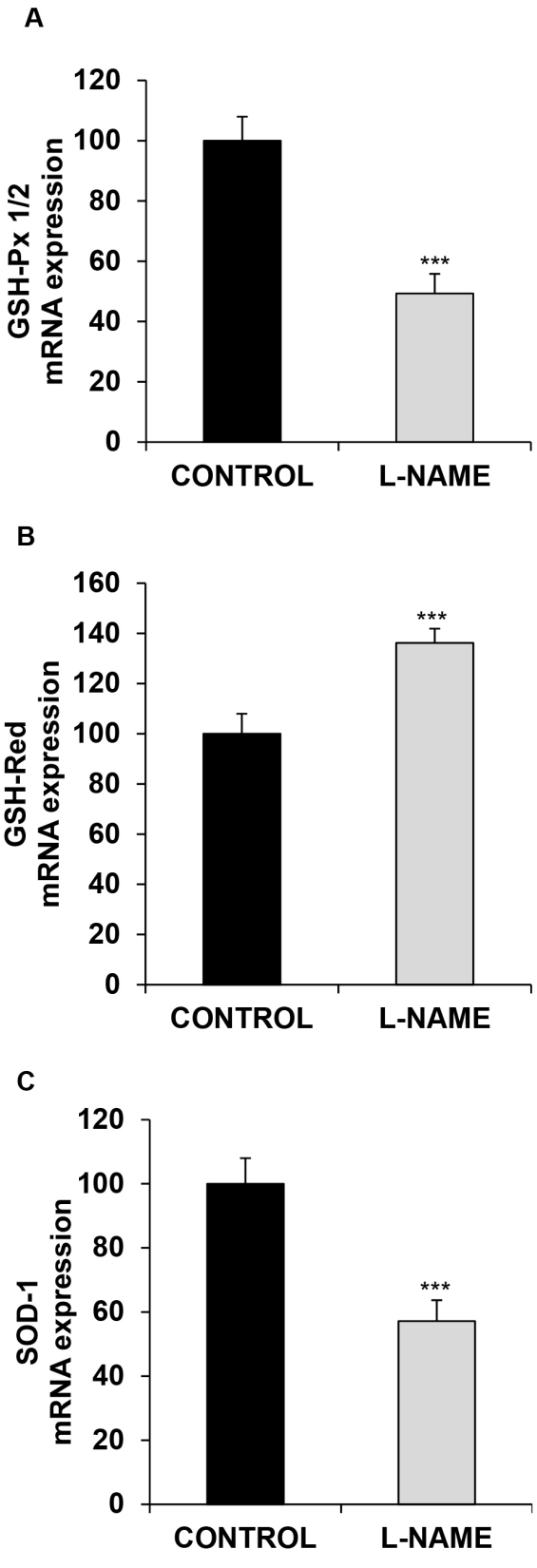

Figure 4. Gene expression of antioxidant enzymes. Relative mRNA expression of (**A**) *GSH-Px 1/2*, (**B**) *GSH-Red*, and (**C**) *SOD-1*, in the eyes of normotensive (CONTROL) and hypertensive (Nω-nitro-L-arginine methyl ester, L-NAME) rats. The quantitative fold changes in gene expression were determined relative to *GAPDH* in each corresponding group and calculated using the $2^{-\Delta\Delta Ct}$ formula. Values are expressed as mean ± standard error of the mean (SEM) of seven animals per group: ***p<0.001 versus the CONTROL group.

the expression of GSH-Red, in the L-NAME-treated rats (Figure 7B).

DISCUSSION

In agreement with previous reports, the administration of L-NAME had no effect on the animals' bodyweight [30,40,41]. However, as expected based on previous studies performed in our laboratory [39], L-NAME induced a significant and sustained elevation of SBP from the first week of treatment (Figure 1).

Thinner GCL, ONL, OS, and RPE/CH layers were observed in the L-NAME group compared with the normotensive animals. Reduced retinal thickness was previously reported in spontaneously hypertensive rats (SHRs) [42,43], mainly in the outer retinal layers [44]. Similar findings have been reported in hypertensive patients without previous ocular abnormalities, thus suggesting a possible association between arterial sclerosis and vascular contraction due to high intravascular pressure in the choroid [45] and a decrease in the retinal blood flow [46].

Several studies highlighting the relevance of NADPH oxidase enzyme in the pathophysiology of AH have reported enhanced activity of this element in hypertensive subjects and in experimental models of hypertension [39,40]. The augmented NADPH oxidase activity observed in the present study in the eyes of the hypertensive rats is in line with previous observations in other organs, including the heart [47-49], liver [47], and kidney [39], as well as in renal tubular

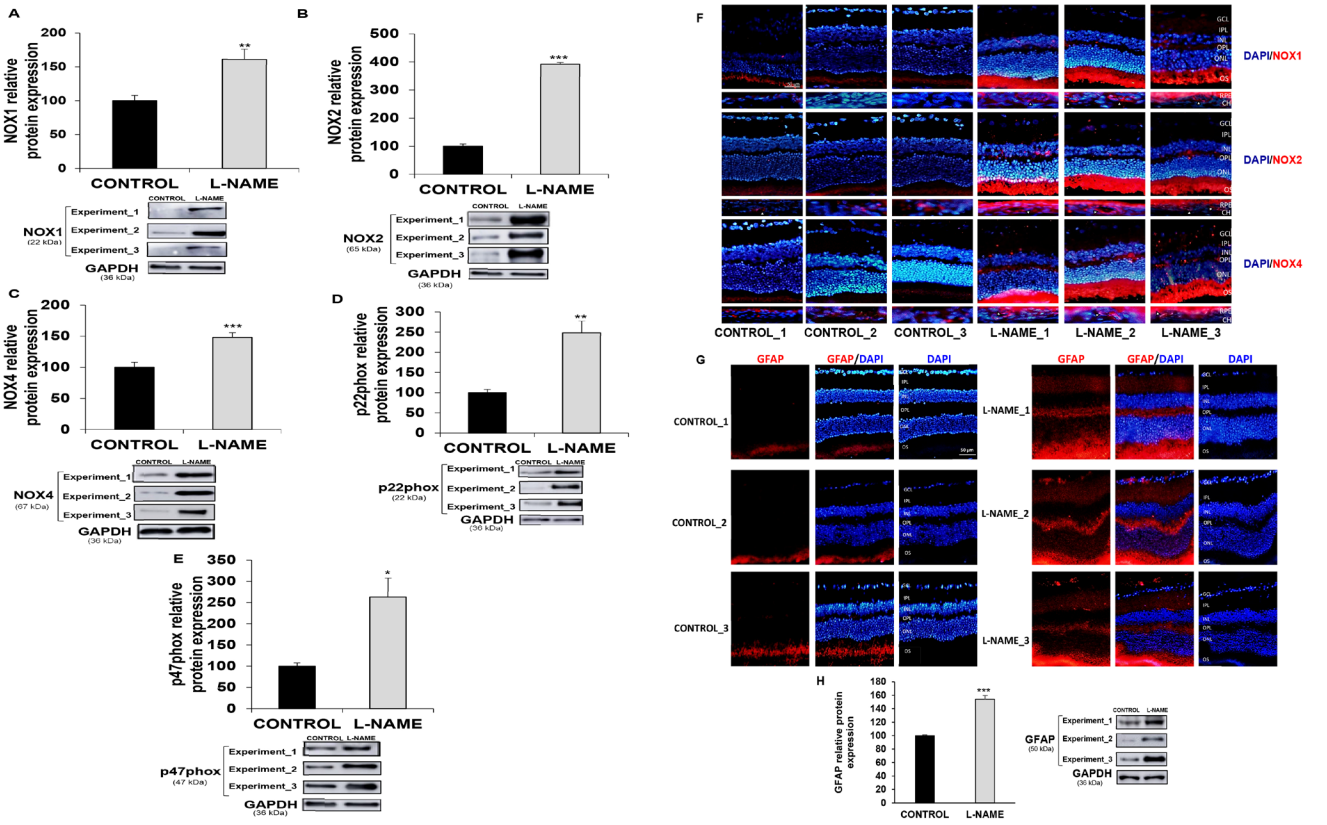

Figure 5. Expresion of nitric oxide synthases and protein tyrosine nitration. Relative protein expression of (**A**) NOX1, (**B**) NOX2, (**C**) NOX4, (**D**) p22phox, and (**E**) p47phox, in eyecup homogenates, and (**H**) GFAP in retinas from normotensive (CONTROL) and hypertensive (Nω-nitro-L-arginine methyl ester, L-NAME) rats. The quantitative fold changes in protein expression were determined relative to GAPDH protein levels in each corresponding group. Plotted values are expressed as mean ± standard error of the mean (SEM) of seven animals per group. *p<0.05, **p<0.01, ***p<0.001 versus the CONTROL group. **F**: Double-immunostaining of nuclei (blue) and NOX isoforms (red; NOX1 (top), NOX2 (middle), and NOX4 (bottom)) proteins in retinal layers and in RPE/choroid layers from control (left column) and L-NAME-treated rats (right column). Arrow heads indicate the presence of NOX proteins mainly around choroidal vessels. Images are representative of four animals per group. **G**: Double immunostaining of nuclei (blue) and GFAP (red) proteins in retinal layers from control (left column) and L-NAME-treated rats (right column). Three immunostained images and western blots per group are shown as a representation of all animal samples processed. GCL, ganglion cell layer; IPL, inner plexiform layer; INL, inner nuclear layer; OPL, outer plexiform layer; ONL, outer nuclear layer; OS, outer segments; RPE, retinal pigment epithelium; CH, choroid.

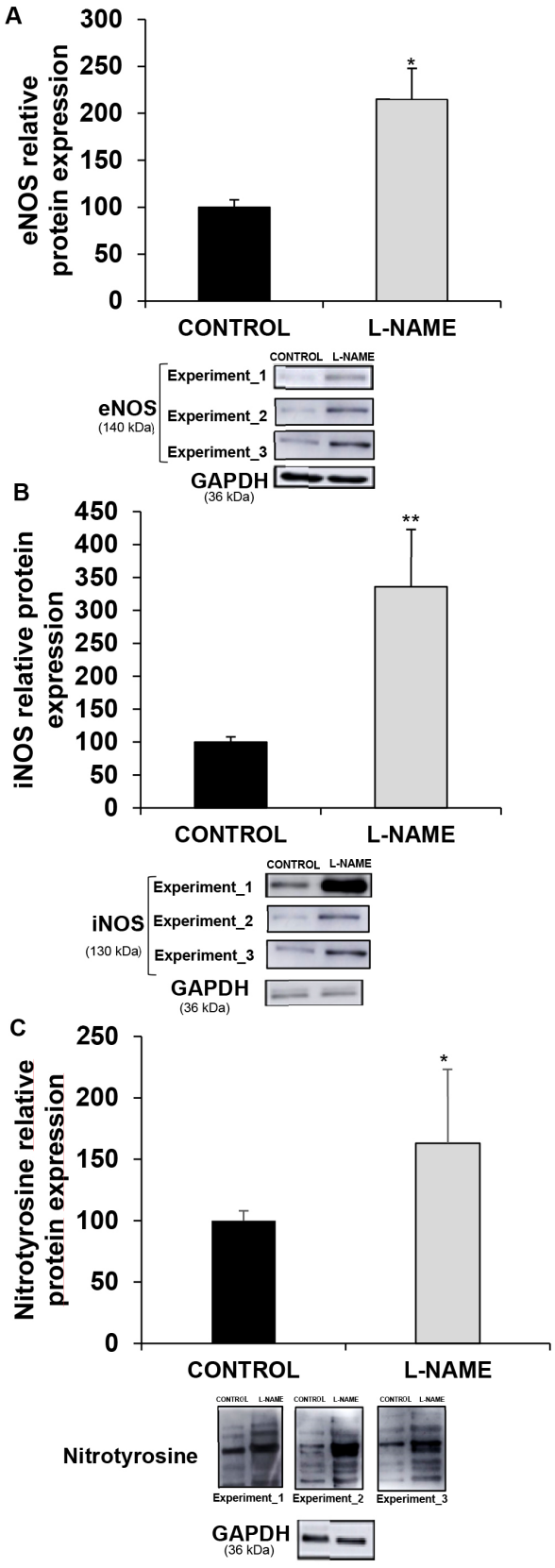

Figure 6. Expresion of nitric oxide synthases and protein tyrosine nitration. Relative protein expression of (**A**) endothelial constitutive nitric oxide synthase (eNOS), (**B**) inflammation inducible nitric oxide synthase (iNOS), and (**C**) nitrotyrosine, in eyecup homogenates from normotensive (CONTROL) and hypertensive (Nω-nitro-L-arginine methyl ester, L-NAME) rats. The quantitative fold changes in protein expression were determined relative to GAPDH protein levels in each corresponding group. Plotted values are expressed as mean ± standard error of the mean (SEM) of seven animals per group, and three western blots per group are shown as a representation of all animal samples processed.*p<0.05, **p<0.01 versus the CONTROL group.

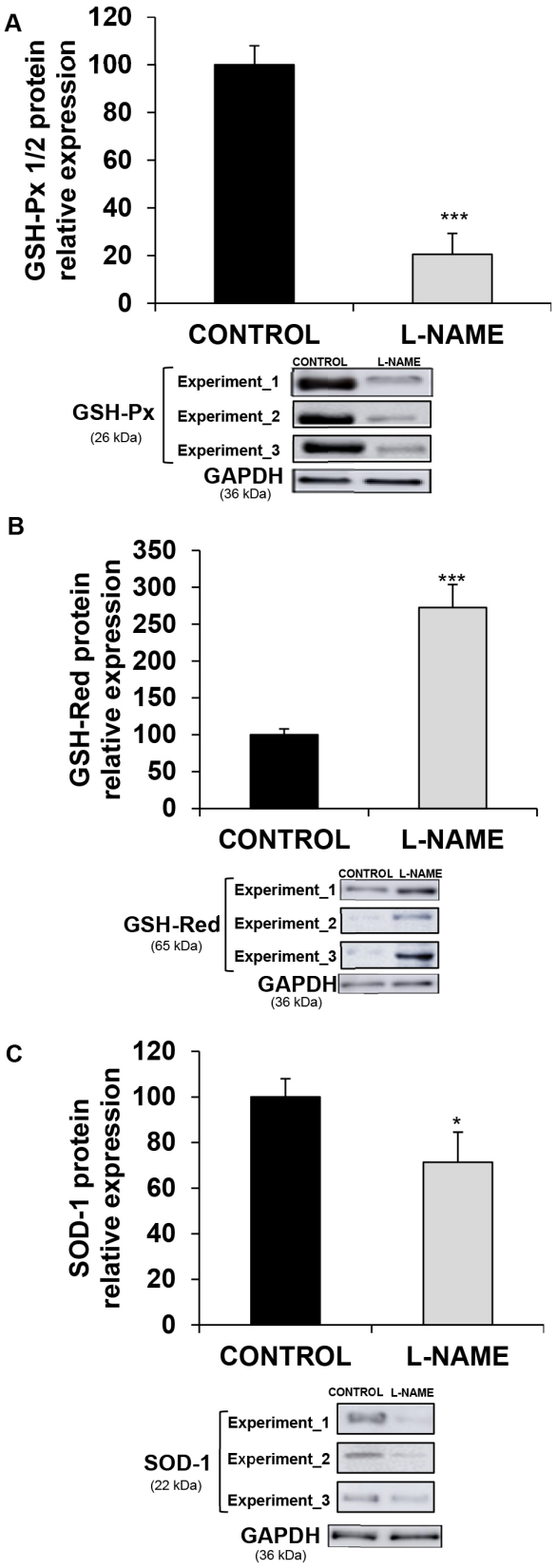

Figure 7. Protein expression of antioxidant enzymes. Relative protein expression of (**A**) GSH-Px 1/2, (**B**) GSH-Red, and (**C**) SOD-1 in eyecup homogenates from normotensive (CONTROL) and hypertensive (Nω-nitro-L-arginine methyl ester, L-NAME) rats. The quantitative fold changes in protein expression were determined relative to the GAPDH protein levels in each corresponding group. Plotted values are expressed as mean ± standard error of the mean (SEM) of seven animals per group, and three western blots per group are shown as a representation of all animal samples processed. *p<0.05, ***p<0.001 versus control group.

cells in different prohypertensive environments [36,38], or in phagocyte cells from hypertensive patients [50].

We confirmed that NADPH oxidase was responsible for the rise of superoxide anion under the experimental conditions (i.e., following L-NAME chronic exposure) with the inhibitory effect of DPI on the luminometer readings. Conversely, coincubation with other inhibitors, such as rotenone (which counteracts the mitochondrial respiratory chain) and oxypurinol (a prototypical inhibitor of xanthine oxidase enzyme) did not modify the chemiluminescence signal. The increased NADPH oxidase activity observed in the hypertensive animals was mainly correlated with higher $O_2^{\cdot-}$ production in the GCL, INL, and ONL of the retina.

Sicard and coworkers reported increased activity of NADPH oxidase in retinal cells of SHRs [51], with an increase in the content of $O_2^{\cdot-}$ in the GCL and no changes in photoreceptors and bipolar cells in the retinas of SHRs when compared with normotensive rats. Furthermore, Pinto et al. showed an increase in superoxide anion production in retinas from SHRs [52]. We might extrapolate that the hyperactivity of this $O_2^{\cdot-}$-generating enzyme in the eyecups of the L-NAME-treated hypertensive rats could be related to the presence of retinal cells in the homogenates. In addition, other eye regions, such as the choroid or the cornea, cannot be excluded as targets of L-NAME-dependent overexpression of NADPH oxidase, due to the demonstrated elevation or presence of the enzyme in these ocular layers [53].

In addition to arterial hypertension, several laboratories have postulated a role for NOX family proteins in the development of different ocular pathologies, for example, retinal vasculitis [54], ischemic retinopathy [55], choroidal neovascularization [23], and diabetes-induced retinal and choroidal vascular injuries [56,57]. The importance of NADPH oxidase has also been highlighted in tissue dysfunction, including the eye in different pathological conditions [17-22,24].

The present data show the first evidence of the location and the protein and gene expression of NOX isoforms and subunits in the hypertensive eye. Thus, the present results indicate that NOX1, NOX2, and NOX4 proteins are detected with abnormally high intensity in retinal layers of L-NAME-treated hypertensive rats, mainly in the outer segment and outer and inner plexiform layers, and that these NADPH oxidase isoforms are also upregulated at the transcriptional level in the eyecups of these rats. Roehlecke et al. [58] reported immunolocalization of NOX2 and NOX4 in the OS from mouse retinas subjected to blue light irradiation. NADPH isoforms are also overexpressed in other target organs affected by hypertension [36,39,59], as well as in other oxidative stress-related systemic pathologies affecting the eye, such as diabetes [17]. In addition, the present findings were matched by a high immunofluorescence signal of GFAP in the plexiform layers from the hypertensive animals; this observation might reflect microglial activation locally in the retina and indicate an unspecific response derived from early retinal damage. In agreement with the present results, microglial activation was previously reported in the retina from spontaneously hypertensive rats when compared with normotensive animals [28].

Multiple ocular pathologies, such as retinopathies (including AMD) [7], glaucoma [5], cataract [2] and choroidal vascular diseases [6], have thus far been related to hypertensive status. The present findings highlight that the abnormally high release of superoxide anions by NADPH oxidase system is a major component of the oxidative damage and the proinflammatory status surrounding hypertension-related ocular diseases. Nevertheless, previous studies using retinas from SHRs did not find any changes in the protein expression of NOX4 and gp91phox when compared with WKY rats, suggesting that the observed increase in the superoxide anion might be due to mitochondrial dysfunction [52].

Concerning the oxidative defense capacity in the present study experimental conditions, we observed downregulation of SOD-1 and GSH-Px 1/2, at the protein and mRNA levels, together with an increase in the expression of GSH-Red, in the eyecups of the hypertensive animals when compared to the normotensive controls. Similar results were recently obtained in the rat lenses of fructose-fed hypertensive rats [60]. The reduction in SOD-1 and GSH-Px 1/2 expression in the eyes from the L-NAME-treated rats might be responsible for an increase in ROS, because the SOD enzyme is in charge of the production of $O_2^{\cdot-}$ from H_2O_2, whereas the GSH-Px enzyme catalyzes the reduction of H_2O_2 to H_2O and O_2, at the expense of reduced GSH. However, the observed increase in GSH-Red might indicate possible compensation to supply GSH, the main component in the antioxidant defense, from oxidized glutathione (GSSG), as it was observed in retinas from SHRs [52]. This hypothesis is confirmed by the enhanced levels of nitrotyrosine (another oxidative stress marker) found in the L-NAME model of hypertension; it is known that $O_2^{\cdot-}$ can react with NO to form peroxynitrite, which modifies free or protein-bound tyrosine residues to form nitrotyrosine. The present results are in line with those by Pinto et al. and Mohamed et al., who reported an enhancement in nitrotyrosine levels in retinas from SHRs, together a rise in lipid peroxides [52,61].

Different ocular pathologies associated with oxidative stress present with alterations in antioxidant enzymes. In this sense, the levels of SOD were significantly lower in patients

with myopia [62], while similar studies have recently reported an increase in SOD and GSH-Px in patients with chronic glaucoma [63]. Modifications in the antioxidant enzyme system have been also found in AMD [64]. These alterations in the availability of antioxidant enzymes might result from local increases in oxidative stress. Nevertheless, the ultimate implications of elevated levels of antioxidant enzymes in the eye are currently unpredictable due to the complexity of the biochemical pathways involved [65], and certainly merit future investigation.

In agreement with previous studies on diabetic retinopathy [66], glaucoma [67,68], and AMD [69,70], the present results also showed that endothelial and inducible isoforms of nitric oxide synthase enzyme were upregulated in rats undergoing L-NAME treatment. Specifically, iNOS overexpression might be due to the existence of an inflammatory process in the eye during the development of arterial hypertension, as has been suggested in eye inflammatory diseases, including AMD [70], uveitis [71], and dry eye disease [72]. Moreover, upregulation of eNOS might represent cellular adaptation of the eye in response to changes in NO availability. Taken together, all these results suggest that activation of NADPH oxidase and $O_2^{\cdot-}$-derived oxidative stress associated with altered metabolism of nitric oxide may affect the ocular vasculature and promote the occurrence of ocular pathologies [16].

Although the alterations in oxidative stress and microglial activation observed in this model of arterial hypertension are currently unknown to induce damage in ocular function, changes in retinal morphology were observed in the L-NAME-treated animals, which might suggest alterations in the hypertensive fundus. Interestingly, Sicard et al. [51] found alterations in retinal function (e.g., abnormally decreased electroretinogram b-wave amplitudes) in spontaneously hypertensive rats, which matched the increase in superoxide content found in these animals in the ganglion cell layer of the retina. In addition, recent studies on eye fundal exploration in animals with a history of normal pregnancy exposed to L-NAME showed narrowed retinal vessels, opacification of the arteriolar wall, increased and diffused optic discs, and slight hemorrhages when compared with control pregnant rats [31]. Whether these (or other) functional alterations are also present in the present experimental model of hypertension is an interesting issue that certainly warrants further research.

Conclusions: The present study demonstrated that arterial hypertension occurs with changes in retinal morphology and increased NADPH oxidase–derived oxidative stress and inflammation in ocular tissues, with special attention paid to the retinal layers and the choroid. There is existing evidence that involves the ROS-generating enzyme NADPH oxidase in the pathophysiological mechanisms contributing to the progression of eye diseases. ROS overproduction in hypertensive rats was accompanied by alterations in the levels of nitric oxide synthase, antioxidant enzymes, and GFAP-revealed microglial activation locally in the eye, thus suggesting an interplay among NADPH oxidase, oxidative stress, inflammation, and hypertensive ocular disease. These findings strengthen the importance of this ROS-generating enzyme system in the oxidative and inflammatory pathogenesis of eye hypertensive diseases.

ACKNOWLEDGMENTS

We thank technical support from Centro de Innovación, Tecnología e Innovación de la Universidad de Sevilla (CITIUS, Servicio de Biología, Servicio de Microscopía). **Author Contribution**: Study design and data management: AM, CMV; data acquisition: AS, CR-G, CF-B, AJB; draft/revision of the article: AS, AJB, HA, AM, CMV. **Funding**: This study was supported by Consejería de Conocimiento, Investigación y Universidad, Junta de Andalucía (2020/275). AS is recipient of an FPU predoctoral fellowship from Ministerio de Ciencia, Innovación y Universidades (FPU17/03465). CR-G was supported by Ministerio de Ciencia, Innovación y Universidades, Ayudas para la Promoción de Empleo Joven e Implantación de la Garantía Juvenil en I+D+i 2017–2020 (PEJ2018–004474-A and CF-B Programa Operativo de Empleo Juvenil 2014–2020 (PEJ2017–399).

REFERENCES

1. Oduntan OA, Masige KP. A review of the role of oxidative stress in the pathogenesis of eye diseases. African Vis Eye Heal. 2011; 70:191-9. .
2. Yu X, Lyu D, Dong X, He J, Yao K. Hypertension and risk of cataract: A meta-analysis. PLoS One 2014; 9:e114012- [PMID: 25474403].
3. Khan SA, Choudhary R, Singh A, Bodakhe SH. Hypertension potentiates cataractogenesis in rat eye through modulation of oxidative stress and electrolyte homeostasis. J Curr Ophthalmol. 2016; 28:123-30. [PMID: 27579456].
4. Cao Y, Li X, Shi P, Wang LX, Sui ZG. Effects of L-carnitine on high glucose-induced oxidative stress in retinal ganglion cells. Pharmacology 2014; 94:123-30. [PMID: 25247444].
5. Langman MJS, Lancashire RJ, Cheng KK, Stewart PM. Systemic hypertension and glaucoma: Mechanisms in common and co-occurrence. Br J Ophthalmol 2005; 89:960-3. [PMID: 16024843].
6. Fraser-Bell S, Symes R, Vaze A. Hypertensive eye disease: a review. Clin Experiment Ophthalmol 2017; 45:45-53. [PMID: 27990740].

7. Miyazaki M, Nakamura H, Kubo M, Kiyohara Y, Oshima Y, Ishibashi T, Nose Y. Risk factors for age related maculopathy in a Japanese population: The Hisayama study. Br J Ophthalmol 2003; 87:469-72. [PMID: 12642312].

8. Bhargava M, Ikram MK, Wong TY. How does hypertension affect your eyes? J Hum Hypertens 2012; 26:71-83. [PMID: 21509040].

9. Small HY, Migliarino S, Czesnikiewicz-Guzik M, Guzik TJ. Hypertension: Focus on autoimmunity and oxidative stress. Free Radic Biol Med 2018; 125:104-15. [PMID: 29857140].

10. Camargo LL, Harvey AP, Rios FJ, Tsiropoulou S, Da Silva RDNO, Cao Z, Graham D, McMaster C, Burchmore RJ, Hartley RC, Bulleid N, Montezano AC, Touyz RM. Vascular nox (NADPH Oxidase) compartmentalization, protein hyperoxidation, and endoplasmic reticulum stress response in hypertension. Hypertension 2018; 72:235-46. [PMID: 29844144].

11. García-Redondo AB, Aguado A, Briones AM, Salaices M. NADPH oxidases and vascular remodeling in cardiovascular diseases. Pharmacol Res 2016; 114:110-20. [PMID: 27773825].

12. Nguyen MVC, Zhang L, Lhomme S, Mouz N, Lenormand J-L, Lardy B, Morel F. Recombinant Nox4 cytosolic domain produced by a cell or cell-free base systems exhibits constitutive diaphorase activity. Biochem Biophys Res Commun 2012; 419:453-8. [PMID: 22326263].

13. Touyz RM, Anagnostopoulou A, Camargo LL, Rios FJ, Montezano AC. Vascular Biology of Superoxide-Generating NADPH Oxidase 5—Implications in Hypertension and Cardiovascular Disease. Antioxid Redox Signal 2019; 30:1027-40. [PMID: 30334629].

14. Brandes RP, Weissmann N, Schröder K. Nox family NADPH oxidases: Molecular mechanisms of activation. Free Radic Biol Med 2014; 76:208-26. [PMID: 25157786].

15. Toda N, Nakanishi-Toda M. Nitric oxide: Ocular blood flow, glaucoma, and diabetic retinopathy. Prog Retin Eye Res 2007; 26:205-38. [PMID: 17337232].

16. Opatrilova R, Kubatka P, Caprnda M, Büsselberg D, Krasnik V, Vesely P, Saxena S, Ruia S, Mozos I, Rodrigo L, Kruzliak P, dos Santos KG. Nitric oxide in the pathophysiology of retinopathy: evidences from preclinical and clinical researches. Acta Ophthalmol 2018; 96:222-31. [PMID: 28391624].

17. Kowluru A, Kowluru RA. Phagocyte-like NADPH oxidase [Nox2] in cellular dysfunction in models of glucolipotoxicity and diabetes. Biochem Pharmacol 2014; 88:275-83. [PMID: 24462914].

18. Appukuttan B, Ma Y, Stempel A, Ashander LM, Deliyanti D, Wilkinson-Berka JL, Smith JR. Effect of NADPH oxidase 1 and 4 blockade in activated human retinal endothelial cells. Clin Experiment Ophthalmol 2018; 46:652-60. [PMID: 29360265].

19. Singh L, Saini N, Pushker N, Sen S, Sharma A, Kashyap S. Prognostic significance of NADPH oxidase-4 as an indicator of reactive oxygen species stress in human retinoblastoma. Int J Clin Oncol 2016; 21:651-7. [PMID: 26857459].

20. Li J, Wang JJ, Zhang SX. NADPH oxidase 4-derived H2O2 promotes aberrant retinal neovascularization via activation of VEGF receptor 2 pathway in oxygen-induced retinopathy. J Diabetes Res 2015; 2015:1-13. [PMID: 25866826].

21. Jarrett SG, Boulton ME. Consequences of oxidative stress in age-related macular degeneration. Mol Aspects Med 2012; 33:399-417. [PMID: 22510306].

22. Wang H, Fotheringham L, Wittchen ES, Hartnett ME. Rap1 GTPase inhibits tumor necrosis factor-α-induced choroidal endothelial migration via NADPH oxidase- and NF-κB-dependent activation of Rac1. Am J Pathol 2015; 185:3316-25. [PMID: 26476350].

23. Yanai R, Chen S, Uchi S-H, Nanri T, Connor KM, Kimura K. Attenuation of choroidal neovascularization by dietary intake of ω-3 long-chain polyunsaturated fatty acids and lutein in mice. PLoS One 2018; 13:e0196037-[PMID: 29694386].

24. Wang H, Hartnett ME. Roles of nicotinamide adenine dinucleotide phosphate (NADPH) oxidase in angiogenesis: isoform-specific effects. Antioxidants 2017; 6:40-[PMID: 28587189].

25. O'Brien WJ, Krema C, Heimann T, Zhao H. Expression of NADPH oxidase in rabbit corneal epithelial and stromal cells in culture. Invest Ophthalmol Vis Sci 2006; 47:853-63. [PMID: 16505017].

26. Chan EC, van Wijngaarden P, Chan E, Ngo D, Wang J-H, Peshavariya HM, Dusting GJ, Liu G-S. NADPH oxidase 2 plays a role in experimental corneal neovascularization. Clin Sci 2016; 130:683-96. [PMID: 26814205].

27. Altmann C, Schmidt MHH. The Role of Microglia in Diabetic Retinopathy: Inflammation, Microvasculature Defects and Neurodegeneration. Int J Mol Sci 2018; 19:110-[PMID: 29301251].

28. Malchiodi-Albedi F, Matteucci A, Bernardo A, Minghetti L. PPAR-, Microglial Cells, and Ocular Inflammation: New Venues for Potential Therapeutic Approaches. PPAR Res 2008; 2008:295784-[PMID: 18382616].

29. Nagano K, Ishida J, Unno M, Matsukura T, Fukamizu A. Apelin elevates blood pressure in ICR mice with L-NAME-induced endothelial dysfunction. Mol Med Rep 2013; 7:1371-5. [PMID: 23525196].

30. Dornas WC, Silva ME. Animal models for the study of arterial hypertension. J Biosci 2011; 36:731-7. [PMID: 21857120].

31. Ramírez-Montero C, Lima-Gómez V, Anguiano-Robledo L, Hernández-Campos ME, López-Sánchez P. Preeclampsia as predisposing factor for hypertensive retinopathy: Participation by the RAAS and angiogenic factors. Exp Eye Res 2020; 193:107981-[PMID: 32088240].

32. Kiel JW, Reitsamer HA, Walker JS, Kiel FW. Effects of Nitric Oxide Synthase Inhibition on Ciliary Blood Flow, Aqueous Production and Intraocular Pressure. Exp Eye Res 2001; 73:355-64. [PMID: 11520110].

33. Cammalleri M, Dal Monte M, Locri F, Lardner E, Kvanta A, Rusciano D, André H, Bagnoli P. Efficacy of a Fatty Acids

Dietary Supplement in a Polyethylene Glycol-Induced Mouse Model of Retinal Degeneration. Nutrients 2017; 9:1079-[PMID: 28961167].

34. Wilding LA, Uchihashi M, Bergin IL, Nowland MH. Enucleation for treating rodent ocular disease. J Am Assoc Lab Anim Sci 2015; 54:328-32. [PMID: 26045460].

35. Bradford MM. A rapid and sensitive method for the quantitation of microgram quantities of protein utilizing the principle of protein-dye binding. Anal Biochem 1976; 72:248-54. [PMID: 942051].

36. Blanca AJ, Ruiz-Armenta MV, Zambrano S, Miguel-Carrasco JL, González-Roncero FM, Fortuño A, Revilla E, Mate A. Vázquez CM. L-Carnitine ameliorates the oxidative stress response to angiotensin II by modulating NADPH oxidase through a reduction in protein kinase c activity and NF-κB translocation to the nucleus. Food Chem 2017; 228:356-66. [PMID: 28317735].

37. Sasaki M, Ozawa Y, Kurihara T, Kubota S, Yuki K, Noda K, Kobayashi S, Ishida S, Tsubota K. Neurodegenerative influence of oxidative stress in the retina of a murine model of diabetes. Diabetologia 2010; 53:971-9. [PMID: 20162412].

38. Blanca AJ, Ruiz-Armenta MV, Zambrano S, Salsoso R, Miguel-Carrasco JL, Fortuño A, Revilla E, Mate A, Vázquez CM. Leptin induces oxidative stress through activation of NADPH oxidase in renal tubular cells: Antioxidant effect of L-carnitine. J Cell Biochem 2016; 117:2281-8. [PMID: 26918530].

39. Zambrano S, Blanca AJ, Ruiz-Armenta MV, Miguel-Carrasco JL, Revilla E, Santa-María C, Mate A, Vázquez CM. The renoprotective effect of L-carnitine in hypertensive rats is mediated by modulation of oxidative stress-related gene expression. Eur J Nutr 2013; 52:1649-59. [PMID: 23223967].

40. Gómez-Guzmán M, Jiménez R, Sánchez M, Romero M, O'valle F, Lopez-Sepulveda R, María Quintela A, Galindo P, Zarzuelo MJ, Bailón E, Delpón E, Perez-Vizcaino F, Duarte J. Chronic (2) -epicatechin improves vascular oxidative and inflammatory status but not hypertension in chronic nitric oxide-deficient rats. Br J Nutr 2011; 106:1337-48. [PMID: 21910946].

41. Zambrano S, Blanca AJ, Ruiz-Armenta MV, Miguel-Carrasco JL, Arévalo M, Vázquez MJ, Mate A. Vázquez CM. L-Carnitine protects against arterial hypertension-related cardiac fibrosis through modulation of PPAR-γ expression. Biochem Pharmacol 2013; 85:937-44. [PMID: 23295156].

42. Sabbatini M, Tomassoni D, Di Tullio MA, Amenta F. Neuroprotective effect of treatment with calcium antagonists on hypertensive retina. Clin Exp Hypertens 2002; 24:727-40. [PMID: 12450247].

43. Wang S, Ye Q, Tu J, Zhang M, Ji B. Curcumin protects against hypertension aggravated retinal ischemia/reperfusion in a rat stroke model. Clin Exp Hypertens 2017; 39:711-7. [PMID: 28678631].

44. Li Y, Wang Q, Muir ER, Kiel JW, Duong TQ. Retinal Vascular and Anatomical Features in the Spontaneously Hypertensive Rat. Curr Eye Res 2020; 45:1422-9. [PMID: 32255364].

45. Akay F, Gundogan FC, Yolcu U, Toyran S, Uzun S. Choroidal thickness in systemic arterial hypertension. Eur J Ophthalmol 2015; 26:152-7. [PMID: 26350985].

46. Lim H. Bin, Lee MW, Park JH, Kim K, Jo YJ, Kim JY. Changes in Ganglion Cell–Inner Plexiform Layer Thickness and Retinal Microvasculature in Hypertension: An Optical Coherence Tomography Angiography Study. Am J Ophthalmol 2019; 199:167-76. [PMID: 30502337].

47. Gómez-Amores L, Mate A, Revilla E, Santa-María C, Vázquez CM. Antioxidant activity of propionyl-L-carnitine in liver and heart of spontaneously hypertensive rats. Life Sci 2006; 78:1945-52. [PMID: 16263137].

48. Miguel-Carrasco JL, Zambrano S, Blanca AJ, Mate A, Vázquez CM. Captopril reduces cardiac inflammatory markers in spontaneously hypertensive rats by inactivation of NF-kB. J Inflamm (Lond) 2010; 7:21-[PMID: 20462420].

49. Calabró V, Litterio MC, Fraga CG, Galleano M, Piotrkowski B. Effects of quercetin on heart nitric oxide metabolism in L-NAME treated rats. Arch Biochem Biophys 2018; 647:47-53. [PMID: 29621523].

50. San José G, Fortuño A, Beloqui Ó, Díez J, Zalba G. NADPH oxidase CYBA polymorphisms, oxidative stress and cardiovascular diseases. Clin Sci 2008; 114:173-82. [PMID: 18184111].

51. Sicard P, Acar N, Grégoire S, Lauzier B, Bron A, Creuzot-Garcher C, Bretillon L, Vergely C, Rochette L. Influence of rosuvastatin on the NAD(P)H oxidase activity in the retina and electroretinographic response of spontaneously hypertensive rats. Br J Pharmacol 2007; 151:979-86. [PMID: 17572703].

52. Pinto CC, Silva KC, Biswas SK, Martins N, Lopes De Faria JB, Lopes De Faria JM. Arterial hypertension exacerbates oxidative stress in early diabetic retinopathy. Free Radic Res 2007; 41:1151-8. [PMID: 17886037].

53. O'Brien WJ, Heimann T, Rizvi F. NADPH oxidase expression and production of superoxide by human corneal stromal cells. Mol Vis 2009; 15:2535-43. [PMID: 19997580].

54. Al-Shabrawey M, Rojas M, Sanders T, Behzadian A, El-Remessy A, Bartoli M, Parpia AK, Liou G, Caldwell RB. Role of NADPH oxidase in retinal vascular inflammation. Invest Ophthalmol Vis Sci 2008; 49:3239-44. [PMID: 18378574].

55. Al-Shabrawey M, Bartoli M, El-Remessy AB, Platt DH, Matragoon S, Behzadian MA, Caldwell RW, Caldwell RB. Inhibition of NAD(P)H oxidase activity blocks vascular endothelial growth factor overexpression and neovascularization during ischemic retinopathy. Am J Pathol 2005; 167:599-607. [PMID: 16049343].

56. Rojas M, Zhang W, Xu Z, Lemtalsi T, Chandler P, Toque HA, Caldwell RW, Caldwell RB. Requirement of NOX2 expression in both retina and bone marrow for diabetes-induced retinal vascular injury. PLoS One 2013; 8:84357-[PMID: 24358357].

57. Wang H, Jiang Y, Shi D, Quilliam LA, Chrzanowska-Wodnicka M, Wittchen ES, Li DY, Hartnett ME. Activation of Rap1 inhibits NADPH oxidase-dependent ROS generation in retinal pigment epithelium and reduces choroidal neovascularization. FASEB J 2014; 28:265-74. [PMID: 24043260].

58. Roehlecke C, Schumann U, Ader M, Brunssen C, Bramke S, Morawietz H, Funk RHW. Stress Reaction in Outer Segments of Photoreceptors after Blue Light Irradiation. PLoS One 2013; 8:e71570-[PMID: 24039718].

59. Miguel-Carrasco JL, Monserrat MT, Mate A, Vázquez CM. Comparative effects of captopril and l-carnitine on blood pressure and antioxidant enzyme gene expression in the heart of spontaneously hypertensive rats. Eur J Pharmacol 2010; 632:65-72. [PMID: 20123095].

60. Bodakhe SH, Singh A, Khan SA, Choudhary R. Cinnamaldehyde Attenuates Cataractogenesis via Restoration of Hypertension and Oxidative Stress in Fructose-Fed Hypertensive rats. J Pharmacopuncture. 2016; 19:137-44. [PMID: 27386147].

61. Mohamed IN, Soliman SA, Alhusban A, Matragoon S, Pillai BA, El-Remessy AB, Elmarkaby AA. Diabetes exacerbates retinal oxidative stress, inflammation, and microvascular degeneration in spontaneously hypertensive rats. Mol Vis 2012; 18:1457-66. [PMID: 22736937].

62. Bhatia RP, Rai R, Rao GRK. Role of malondialdehyde and superoxide dismutase in cataractogenesis. Ann Ophthalmol (Skokie) 2006; 38:103-6. [PMID: 17416937].

63. Benoist d'Azy C, Pereira B, Chiambaretta F, Dutheil F. Oxidative and anti-oxidative stress markers in chronic glaucoma: A systematic review and meta-analysis. PLoS One 2016; 11:e0166915-[PMID: 27907028].

64. Tokarz P, Kaarniranta K, Blasiak J. Role of antioxidant enzymes and small molecular weight antioxidants in the pathogenesis of age-related macular degeneration (AMD). Biogerontology 2013; 14:461-82. [PMID: 24057278].

65. Lei XG, Zhu J-H, Cheng W-H, Bao Y, Ho Y-S, Reddi AR, Holmgren A, Arnér ESJ. Paradoxical roles of antioxidant enzymes: basic mechanisms and health implications. Physiol Rev 2016; 96:307-64. [PMID: 26681794].

66. Hernández-Ramírez E, Sánchez-Chávez G, Estrella-Salazar LA, Salceda R. Nitrosative stress in the rat retina at the onset of streptozotocin-induced diabetes. Cell Physiol Biochem 2017; 42:2353-63. [PMID: 28848155].

67. Jeoung JW, Kim DM, Oh S, Lee JS, Park SS, Kim JY. The relation between endothelial nitric oxide synthase polymorphisms and normal tension glaucoma. J Glaucoma 2017; 26:1030-5. [PMID: 28777225].

68. Xiang Y, Dong Y, Li X, Tang X. Association of common variants in eNOS gene with primary open angle glaucoma: A meta-analysis. J Ophthalmol 2016; 2016:1-11. [PMID: 27242919].

69. Bhutto IA, Baba T, Merges C, McLeod DS, Lutty GA. Low nitric oxide synthases (NOSs) in eyes with age-related macular degeneration (AMD). Exp Eye Res 2010; 90:155-67. [PMID: 19836390].

70. Forrester JV. Bowman lecture on the role of inflammation in degenerative disease of the eye. Eye (Lond) 2013; 27:340-52. [PMID: 23288138].

71. Zheng C, Lei C, Chen Z, Zheng S, Yang H, Qiu Y, Lei B. Topical administration of diminazene aceturate decreases inflammation in endotoxin-induced uveitis. Mol Vis 2015; 21:403-11. [PMID: 25883526].

72. You IC, Coursey TG, Bian F, Barbosa FL, de Paiva CS, Pflugfelder SC. Macrophage phenotype in the ocular surface of experimental murine dry eye disease. Arch Immunol Ther Exp (Warsz) 2015; 63:299-304. [PMID: 25772203].

Articles are provided courtesy of Emory University and the Zhongshan Ophthalmic Center, Sun Yat-sen University, P.R. China. The print version of this article was created on 2 April 2021. This reflects all typographical corrections and errata to the article through that date. Details of any changes may be found in the online version of the article.